analytical chemistry

Article

Cite This: Anal. Chem. 2018, 90, 9272−9280

pubs.acs.org/ac

Digestion-Free Analysis of Peptides from 30-year-old Formalin-Fixed, Paraffin-Embedded Tissue by Mass Spectrometry Imaging

Martin R. L. Paine,[†] Shane R. Ellis,[†] Dan Maloney,[§] Ron M. A. Heeren,[†] and Peter D. E. M. Verhaert*[,†,‡]

[†]Maastricht MultiModal Molecular Imaging (M4I) Institute, Division of Imaging Mass Spectrometry, Maastricht University, Universiteitssingel 50, 6229ER Maastricht, The Netherlands

[‡]ProteoFormiX, Janssen Pharmaceutica Campus, Turnhoutseweg 30, B2340 Beerse, Belgium

[§]Bioinformatics Solutions Inc., 470 Weber Street North, Waterloo, Ontario N2L 6J2, Canada

Supporting Information

ABSTRACT: Formalin-fixed neuroendocrine tissues from American cockroaches (*Periplaneta americana*) embedded in paraffin more than 30 years ago were recently analyzed by matrix-assisted laser desorption/ionization mass spectrometry imaging (MALDI-MSI), to reveal the histological localization of more than 20 peptide ions. These represented protonated, and other cationic species of, at least, 14 known neuropeptides. The characterization of peptides in such historical samples was made possible by a novel sample preparation protocol rendering the endogenous peptides readily amenable to MSI analysis. The protocol comprises brief deparaffinization steps involving xylene and ethanol, and is further devoid of conventional aqueous washing, buffer incubations, or antigen retrieval steps. Endogenous secretory peptides that are typically highly soluble are therefore retained in-tissue with this protocol. The method is fully "top-down", that is, without laborious in situ enzymatic digestion that typically disturbs the detection of low-abundance endogenous peptides by MSI. Peptide identifications were supported by accurate mass, on-tissue tandem MS analyses, and by earlier MALDI-MSI results reported for freshly prepared *P. americana* samples. In contrast to earlier literature accounts stating that MALDI-MSI detection of endogenous peptides is possible only in fresh or freshly frozen tissues, or exceptionally, in formalin-fixed, paraffin-embedded (FFPE) material of less than 1 year old, we demonstrate that MALDI-MSI works for endogenous peptides in FFPE tissue of up to 30 years old. Our findings put forward a useful method for digestion-free, high-throughput analysis of endogenous peptides from FFPE samples and offer the potential for reinvestigating archived and historically interesting FFPE material, such as those stored in hospital biobanks.

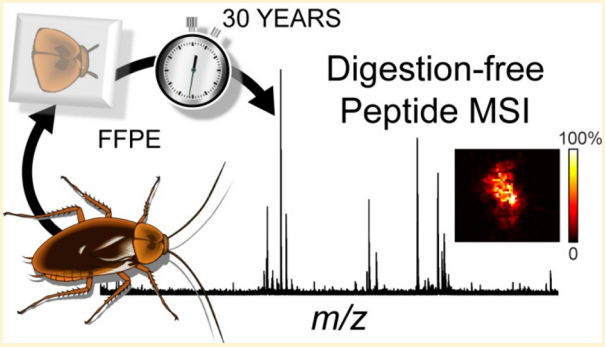

Endogenous peptides represent a subclass of biomolecules that participate in a diverse array of physiological processes within most, if not all, multicellular organisms, including humans. Prominent examples are the peptides produced by the (neuro)endocrine system, but endogenous peptides are known to regulate scores of other molecular activities, ranging from basic processes such as DNA synthesis,[1] to host defense (antimicrobials) in outer epidermal layers.[2,3] To function as extracellular signaling molecules, endogenous peptides are secreted by many different glands as water-soluble messengers acting on membrane receptors on the surface of target cells that in turn cause the release of intracellular secondary messengers.[4] Understanding the (dys-)regulation of these signaling pathways is of great interest in the study of many diseases, endocrine disorders, and sensitivity to pharmaceuticals.[5] To gain further insight into the biochemical changes that occur related to endogenous peptide signaling, analytical techniques are required that can identify different peptide structures and resolve their spatial distribution within biological tissue. Identifying changes in peptide distribution within the tissue is important as peptides may be synthesized in one tissue region and stored/released by another region. This is one of the reasons why genomic or transcriptomic data do not always correlate with proteomic/peptidomic counterparts. For instance, many neuropeptides produced within specific neurosecretory regions of the brain are transported to and released from so-called neurohemal sites, such as the pituitary gland, whereas others are produced and secreted from the neurosecretory glands themselves.[6,7]

Mass spectrometry imaging (MSI) is an analytical technique capable of locally detecting hundreds of peptides and proteins based on their differing mass-to-charge (m/z) ratio while simultaneously mapping each molecule's spatial distribution in

Received: April 24, 2018
Accepted: July 5, 2018
Published: July 5, 2018

DOI: 10.1021/acs.analchem.8b01838
Anal. Chem. 2018, 90, 9272−9280

two- and even three-dimensions.[8] Mass spectrometry has been widely utilized in the field of peptidomics and proteomics in both top-down and bottom-up workflows, with both strategies also being applied to imaging modalities. As a significant fraction of protein-centered MSI research is typically carried out in collaboration with histopathologists, tissue samples are prepared using the well-established clinical protocol of tissue fixation with formaldehyde,[9] followed by embedding in paraffin. Formaldehyde (or formalin) fixation crosslinks the proteins in the tissue, helping retain the cell morphology for histological examination and providing long-term preservation. A heat-based and proteolytic antigen retrieval step is typically performed to render tissue samples prepared with this protocol amenable to proteomic analyses. Such bottom-up approaches whereby in situ enzymatic digestion of proteins and peptides is carried out before the MSI analysis has gained widespread application, and it is generally accepted in the field that formaldehyde fixation is incompatible with top-down workflows, that is, to detect intact proteins.[10] The major drawback of using any protocol involving enzymatic digestion, however, is that cleavage of all the proteins into smaller peptide fragments jeopardizes the detection of endogenous peptides present, particularly those of naturally low-abundance as peptide digests may produce isobaric peaks that overlap with endogenous peptides. Moreover, single stage MS has no ability to readily discern endogenous peptides from proteolytic fragments and the digestion step itself introduces added risk of analyte delocalization. In addition, protocols involving antigen retrieval and enzymatic digestion typically involve the use of aqueous solutions at elevated temperatures. For secretory peptides that are hydrophilic in nature, and highly prone to rapid degradation, these conditions can result in chemical alteration/breakdown, delocalization, or complete loss of the peptides from the tissue.[11] It is, therefore, not surprising that the conventional proteomics MSI sample protocol is unfavorable for endogenous (neuro)peptide MSI analysis. This is confirmed by studies from different laboratories reporting that direct, digestion-free, imaging of (endogenous) peptides by MSI straight from formalin-fixed, paraffin-embedded (FFPE) tissues is not possible.[12,13]

When targeting the detection of proteins and endogenous peptides in MSI, multiple studies in various biological tissues have been restricted to fresh tissue preparations,[14−18] freshly frozen preparations,[19−23] or fresh tissues embedded in gelatin and snap-frozen.[24,25] These also include the model system of the present paper, where neuropeptides have been imaged in fresh *P. americana* (retro)cerebral whole mounted tissues and cryosections.[26] Thus far, there has been only one report of digestion-free imaging of endogenous peptides by MSI directly from formalin-fixed, paraffin-embedded (FFPE) tissues. This was a matrix-assisted laser desorption/ionization (MALDI) MSI study investigating the effect of different MALDI matrices and sample preparation (FFPE vs fresh frozen) on the detectability of endogenous peptides and metabolites.[12] One of the conclusions made from the study was the necessity of the use of 2,4-dinitrophenylhydrazine (a "reactive" matrix) to enable endogenous peptides' MALDI detection. In addition, it was reported that endogenous peptides are only detectable from FFPE tissue within 1 year from the time of embedding and then only by incorporating the reactive matrix in the sample preparation.[12] This assertion severely limits the number of samples that would be accessible by digestion-free MSI analysis, as the majority of samples in the many banks of FFPE tissues that exist in hospitals, laboratories, and research institutes around the world are older than 1 year. Therefore, the development of a method that makes FFPE samples older than 1 year compatible with MSI of endogenous peptides would be very advantageous.

With the aim to develop an MSI method capable of detecting endogenous peptides from aged FFPE tissue, we focused on samples of model neuropeptide secreting tissues that were fixed and embedded 31 years prior to analysis.[27] These samples were taken from an insect retrocerebral complex, a neurosecretory tissue serving as a model biological system for neuropeptide secretion of higher-order animals, such as in the mammalian pituitary.[18] We describe a novel MSI sample preparation method for the digestion-free detection of endogenous neuropeptides and its application to >30-year-old FFPE tissue of *P. americana*. The method is free of enzymatic digestion, antigen retrieval, or aqueous washing of the tissue, allowing the label-free detection of endogenous peptides by (MALDI) MSI. These findings demonstrate that the imaging of endogenous peptides by mass spectrometry is possible from FFPE tissues embedded up to 30 years ago thus unlocking the possibility of conducting retrospective studies on endogenous peptides using the plethora of FFPE samples stored by pathologists and histologists all over the world.

EXPERIMENTAL SECTION

Chemicals. HPLC-grade ethanol (dehydrated) was purchased from Biosolve B.V. (Valkenswaard, The Netherlands). Xylene (>99%), HPLC-grade acetonitrile (ACN; >99.93%), 2,5-dihydroxybenzoic acid (DHB; >99.0%), and trifluoracetic acid (TFA; 99%) were purchased from Sigma-Aldrich (Zwijndrecht, The Netherlands).

Animals. In 1986, American cockroaches (*Periplaneta americana* L.) of the same sex and developmental stage (all were adult sexually mature insects) were taken from a stock colony maintained under standard laboratory conditions and provided with dry dog food, oatmeal, and water ad libitum.[27] Retrocerebral complexes, consisting of the corpora cardiaca (CC, both the glandular (CCg) and the storage part (CCs)) and the corpora allata (CA; Figure 1), were dissected, while the tissue was immersed in 4% paraformaldehyde (i.e., 10% formalin). To allow easy handling and forceps manipulation of the tissue for processing into paraffin, the tissue of interest was dissected while still associated with a piece of the underlying foregut (Figure 1a). Following overnight fixation, the tissues were dehydrated and embedded in paraffin as described previously[27] and stored at ambient temperature until their use for MSI in 2017.

Tissue Preparation. In 2017 (i.e., 31 years after formalin fixation and paraffin embedding), the cockroach neuroendocrine tissues were sectioned at 20 μm thickness on a standard microtome (Leica Reichert-Jung 2040 Autocut). A series of ribbons of 10−15 adjacent sections were transferred onto indium tin oxide (ITO)-coated glass slides (3−4 ribbons per slide, 8 in total, representing the entire embedded tissue). The slides were put on a hot plate (50 °C) where the paraffin sections stretched and allowed to air-dry for 30 min, after which they were stored at room temperature until needed. Prior to matrix application, sectioned tissues were deparaffinized using a modified deparaffinization protocol that omits aqueous washing steps. Slides were immersed in xylene (100%; 3 min), fresh xylene (100%; 2 min), ethanol (100%; 2 min), and then fresh ethanol (100%; 1 min). The deparaffinized

DOI: 10.1021/acs.analchem.8b01838
Anal. Chem. 2018, 90, 9272−9280

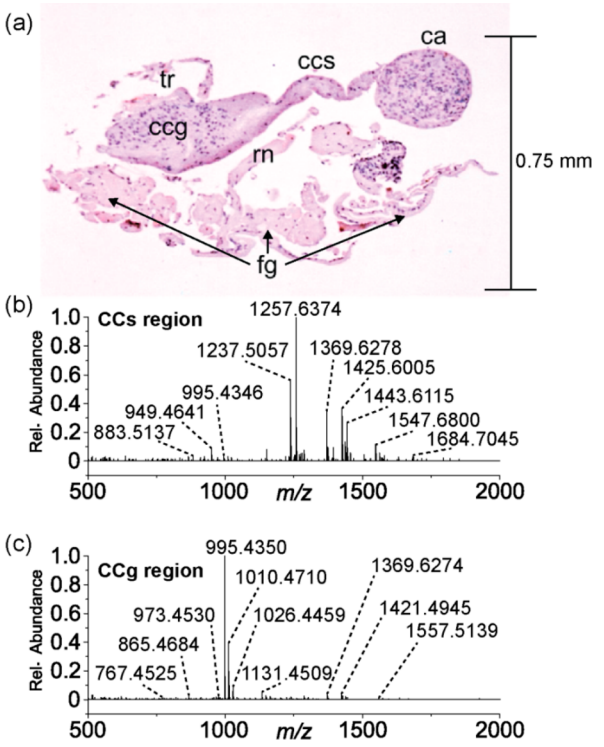

Figure 1. (a) Optical image of an H&E-stained longitudinal histological section of retrocerebral complex of *P. americana*, showing distinct neuroendocrine regions and surrounding tissues. Abbreviations: CA, corpus allatum; CCg, glandular lobe of corpus cardiacum; CCs, storage lobe of corpus cardiacum; fg, foregut epithelium and visceral muscle tissue; rn, recurrent nerve; tr, trachea. Scale bar: 0.75 mm. Positive-ion mode high mass resolution Orbitrap MALDI-MS spectra acquired from a single 20 μm pixel after background subtraction within (b) CCs and (c) CCg regions.

samples were allowed to dry in a fume hood (1−2 min) and then coated with a matrix solution of 2,5-dihydroxybenzoic acid (DHB; 50 mg/mL) in ACN/H_2O/TFA (49.95:49.95:0.1 v/v). The matrix solution was applied as a nebulized spray using a TM sprayer (HTX Technologies, NC, U.S.A.) with the following settings: flow rate, 0.1 mL/min; spray nozzle velocity, 1200 mm/min; spray nozzle temperature, 75 °C; number of passes, 3; nitrogen gas pressure, 10 psi; track spacing, 1 mm; drying time between passes, 10 s.

MALDI MS Imaging Acquisition. Accurate mass measurements were performed on five replicate samples in positive-ion mode in the range of m/z 500−2000 using a hybrid ion trap-Orbitrap mass spectrometer (LTQ Velos Pro Orbitrap Elite, Thermo Fisher Scientific, Bremen, Germany) coupled to an intermediate-pressure MALDI/ESI source based on a dual ion-funnel geometry (Spectroglyph LLC, Kennewick, WA, U.S.A.).[28] Prior to imaging experiments, the instrument was mass calibrated with the Pierce LTQ Velos calibration solution (Thermo Fisher Scientific, Bremen, Germany) using the ESI source. All Orbitrap spectra were acquired at a nominal mass resolution of 120000 fwhm@m/z 400 using a 250 ms injection time. A frequency tripled Nd:YLF laser (349 nm) was operated at 1 kHz, a pulse energy of 1.5 μJ and focused to a ∼15 μm spot. Orbitrap-based MS images were recorded at a spatial resolution of 20 μm. Visualization of data was achieved by converting the raw data into a Matlab-readable format and using in-house-developed Matlab tools for baseline correction and peak picking as recently described.[28,29]

For high-throughput measurements of multiple tissue sections, 26 consecutive sections were analyzed in positive-ion mode using a rapifleX MALDI ToF (time-of-flight) mass spectrometer (Bruker Daltonics, Billerica, MA, U.S.A.). Spectra were acquired in the m/z 500−2000 range with the ToF analyzer operating in reflectron mode. Prior to imaging experiments, the instrument was mass calibrated using the monoisotopic cluster peaks of red phosphorus spotted directly onto the target plate. Imaging experiments were controlled by the flexImaging 4.0 software (Bruker Daltonics, Billerica, MA, U.S.A.) with a laser raster size of 40 μm × 40 μm and a stage motion (i.e., pixel size) of 50 μm × 50 μm. At each pixel position, 200 laser shots were summed to generate a representative spectrum for each pixel, with the digitizer sampling rate at 1.25 GS/s. Data processing, visualization, and coregistration of optical images was performed using the SCiLS Lab software version 2018b (SCiLS GmbH, Bremen, Germany). Mass spectra were preprocessed during import into SCiLS Lab using baseline removal by iterative convolution and root-mean-square (RMS) spectral normalization.[30] For subsequent data analysis, a minimum interval width of 300 mDa around the average peak center was used to account for peak shifts throughout the experiment.

H&E Staining. Sections were recuperated after MSI data recording and poststained with hematoxylin and eosin to facilitate histological recognition of the different cell and tissue types/features. DHB matrix was removed from the sections by a 5 min wash in 70% ethanol, followed by a brief wash in distilled water. Slides were then stained in Harris hematoxylin solution for 8 min, after which they were washed in running tap water for 5 min. Subsequently, sections were counterstained in eosin-phloxine solution for 1 min, followed by conventional dehydration and coverslipping; dehydration through 70% and 96% ethanol (two changes of 5 min each), clearing steps in two changes of xylene (5 min each), and mounting with xylene-based mounting medium.

Data Analysis. Imaging data were subjected to principle component analysis (PCA) and hierarchical cluster analysis using the Matlab-based ChemomeTricks software package (v. 1.51) that provides unsupervised clustering of spatially correlated peaks.[29] Peaks with peptide-like isotopic distribution in clusters showing high spatial correlation with the various tissue regions (aided by visual inspection of H&E stained sections) and thus assumed to be arising from tissue-derived signals, were targeted for further interrogation.

Structural Characterization. Structural assignments of ions were supported by accurate mass measurements from the Orbitrap analyzer and MS/MS measurements following collision-induced dissociation (CID) performed and detected in the ion-trap analyzer for peptides detected at high enough signal (SI, Figure 1). MS/MS spectra were analyzed using the PEAKS DB algorithm included in PEAKS Studio (Version 8.5; BioInformatics Solutions, Waterloo, Canada) for de novo sequencing assisted sequence database interrogation-based protein identification.[31] Sequence validation searches were against a database containing known neuropeptides as well as a subdatabase of all insect proteins contained in the NCBI nonredundant database. Accurate mass assignments were made using a ±3 ppm mass tolerance and an ion-trap fragmentation mass error tolerance of 0.5 Da with a "no enzyme search" selected. The variable modifications selected were pyro-Glu (pQ) from Q, sulfation, and amidation, allowing three variable post-translational modifications per peptide. Peptides with a

DOI: 10.1021/acs.analchem.8b01838
Anal. Chem. 2018, 90, 9272−9280

Table 1. Known *Periplaneta americana* Endogenous Peptides Detected in Tissue Sections of >30 Years Old FFPE American Cockroach Neurohaemal Organs[a]

[trivial name]	sequence	adduct ion	observed m/z	theor. m/z	mass error (ppm)
[proctolin]	RYLPT	$[M + H]^+$	649.3668	649.3668	0.02
[Pea-AST-13]	$RPYNFGL_{amide}$	$[M + H]^+$	865.4685	865.4679	0.69
[Pea-PK-2]	$SPPFAPRL_{amide}$	$[M + H]^+$	883.5157	883.5148	0.96
Pea-K-1	$RPSFNSWG_{amide}$	$[M + H]^+$	949.4642	949.4632	1.05
[Pea-CAH-1]	$pQVNFSPNW_{amide}$	$[M + H]^+$	973.4526	973.4526	−0.04
		$[M + Na]^+$	995.4352	995.4346	0.62
		$[M + K]^+$	1011.4089	1011.4085	0.37
[Pea-CAH-2]	$pQLTFTPNW_{amide}$	$[M + H]^+$	988.4890	988.4886	0.31
		$[M + Na]^+$	1010.4709	1010.4706	0.26
		$[M + K]^+$	1026.4472	1026.4446	2.56
[Pea-PK-3]	$LVPFRPRL_{amide}$	$[M + H]^+$	996.6443	996.6465	−2.31
[Pea-PK-1]	$HTAGFIPRL_{amide}$	$[M + H]^+$	1010.5899	1010.5894	0.48
[Pea-LSK-2]	$pQSDDY(SO_3)GHMRF_{amide}$	$[M + H - SO_3]^+$	1237.5057	1237.5055	0.18
[Pea-LMS]	$pQDVDHVFLRF_{amide}$	$[M + H]^+$	1257.6379	1257.6374	0.33
[corazonin]	$pQTFQYSRGWTN_{amide}$	$[M + H]^+$	1369.6294	1369.6284	0.75
[Pea-SK]	$EQFDDY(SO_3)GHMRF_{amide}$	$[M + H - SO_3]^+$	1443.6122	1443.6110	0.82
[Pea-PK-4]	$DHLPHDVYSPRL_{amide}$	$[M + H]^+$	1447.7478	1447.7441	2.58
[Pea-PK-6]	$SESEVPGMWFGPRL_{amide}$	$[M + H]^+$	1590.7719	1590.7733	0.88

[a]Abbreviations: AST, allatostatin; CAH, cardioacceleratory hormone; K, kinin; LMS, leucomyosuppressin; LSK, leucosulfakinin; PK, pyrokinin; pQ, pyroglutamic acid; SK, sulfakinin.

−10 log P score greater than 20 were considered accurately identified.

RESULTS

The retrocerebral complex of *P. americana* cockroaches, preserved as FFPE samples over 30 years ago, were analyzed by MALDI-MSI. To render the tissues amenable to MSI with minimal perturbation of the endogenous peptides, we developed a new, simplified protocol for sample processing as described in more detail in the methods section. Briefly, samples were placed in a xylene bath twice for the bulk removal of the paraffin, followed by a 100% ethanol bath (twice) to remove the residual xylene and soluble compounds from the tissue maximally reducing its hydrophobicity, and thus rendering it readily miscible with the hydrophilic matrix solution. After the samples were air-dried and coated with DHB matrix, MALDI-MS was performed on the insect retrocerebral complex tissue in positive-ion mode (Figure 1). Because the obtained mass spectra were dominated by matrix cluster peaks, background subtraction was applied, yielding more than 20 peptide signals with high signal-to-noise in the m/z 500−2000 range. Single pixel, background subtracted spectra acquired from the CCs and CCg regions of the retrocerebral complex are shown in Figure 1b and c, respectively.

Verification that MS signals originate from endogenous peptides, rather than from nonpeptide (background) ions, was supported by accurate mass measurements using the Orbitrap mass analyzer at 120000 resolving power setting. Ultimate molecular sequence assignments of the peaks labeled in Figure 1 were based on accurate mass determination and MS/MS fragmentation data from CID tandem MS experiments. A total of 18 of the peptide ion species could be readily identified and assigned to established cockroach neuropeptide sequences (Table 1), consistent with previous reports in literature on MALDI-MS analyses of fresh preparations of *P. americana* tissue. They represent 14 neuropeptides detected as multiple adduct species, being previously detected in the *P. americana* retrocerebral complex by MALDI-MS and sequenced by tandem MS.[26,32] These include hypertrehalosemic hormones, corazonin, sulfakinins, pyrokinins, kinin, and allatostatin. Products from all these neuropeptide precursors are detected throughout the CCs tissue (Figure 1b), including leucomyosuppressin (Pea-LMS), corazonin, the sulfakinins Pea-SK and leucosulfakinin (Pea-LSK-II), kinin (Pea-K-1), and a range of pyrokinins (Pea-PK-1 to Pea-PK-6). The CCg region spectrum (Figure 1c) is dominated by the American cockroach cardioacceleratory hormones I and II (Pea-CAH-1 and Pea-CAH-2).[33] These two hypertrehalosemic hormones are readily detected as Na^+ adducts at m/z 995.4346 and 1010.4709, respectively, an observation also made in previous studies.[18,27]

As illustrated by representative on-tissue, single-pixel mass spectra of the various regions of the retrocerebral complex (Figure 1), many of the observed peaks were detected at low relative abundances, being present at tissue (sub)structures, i.e., specific neurosecretory nerve fiber bundles and neuroendocrine cell groups. The MSI data were processed using PCA to facilitate identification of low-abundance peaks originating from different tissue locations. Using this method, spectral features (i.e., peaks associated with peptide ions) were clustered based on their spatial correlation.

Correlation clustering of principal components 1−6 (Figure 2a) exhibited a bifurcation that separates the "tissue-related" features from many of the features that are associated with background signals, reflecting MALDI matrix ion clusters and other chemical background. The assignment of this cluster to tissue-related features as opposed to background features enables a targeted interpretation of the complex MSI data and is sustained by the two-dimensional false-color images (Figure 2; inset). The false-color images describe the correlation of each pixel to the representative spectrum of the tissue-related feature cluster (Figure 2). Within the main tissue-related branch of the dendrogram, subsets of clustering features register to the main histological parts of orthopteroid insect retrocerebral complexes (Figure 2**c**). These consist of the CCg, the CCs, and the CA regions.[26,34,35] Figures 3**a-c** confirms this

DOI: 10.1021/acs.analchem.8b01838
Anal. Chem. 2018, 90, 9272−9280

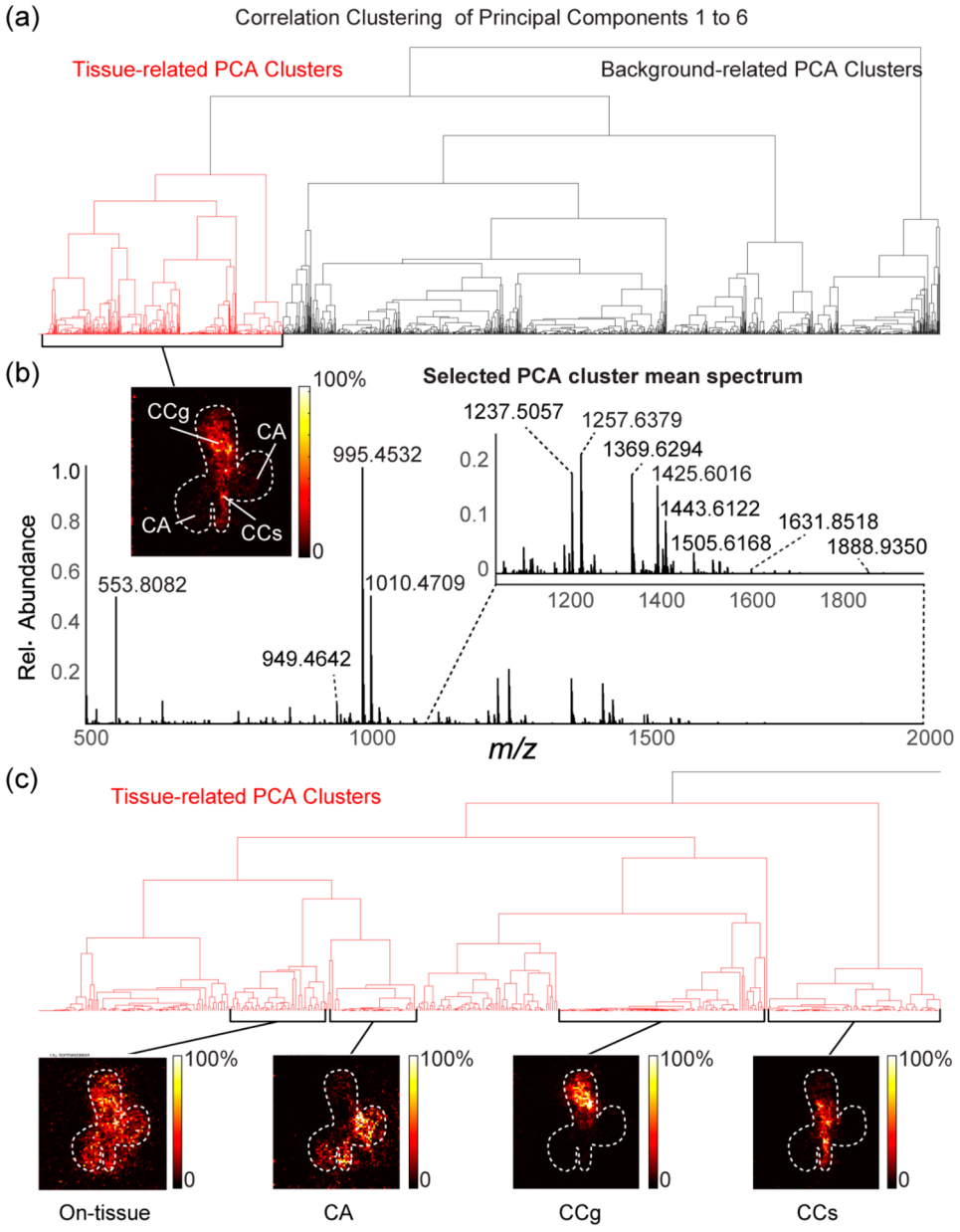

Figure 2. (a) Correlation clustering of principal components 1−6 of a positive-ion mode MALDI-MSI Orbitrap data set of *P. americana* FFPE retrocerebral complex tissue section. (b) Mean spectrum representing selected cluster from (a) showing highest spatial correlation with tissue region based on visual comparison. Insets: associated PCA cluster image showing spatial correlation of spectrum at each pixel position, and magnified subset of spectrum for m/z 1100−2000 range. (c) Subset PCA cluster images showing localized distributions for general "on-tissue" features and three specific neuroendocrine tissue regions: CA, CCg, and CCs.

as mean spectra from each of these clusters display the distinct molecular signature of anatomical regions that include (among others) the endogenous peptides identified in Table 1. As expected, the glandular portion of the corpus cardiacum (CCg, Figure 3a) contains predominantly Pea-CAH-1 and Pea-CAH-2 as sodiated ions at m/z 995.4352 and 1010.4709, respectively. As the tissue transitions into the storage part of the corpus cardiacum (Figure 3b), the two CAH peptides are still present but the relative abundance of corazonin and myotropins such as leucomyosuppressin (Pea-LMS) and sulfakinins (including Pea-SK and Pea-LSK-2) increases. The mean spectrum describing the CA (Figure 3c) is markedly different to those observed for the CCg and CCs. While still containing a significant amount of Pea-LMS and corazonin, a range of pyrokinins are also observed to pass through the CA. This confirms previous immunohistochemical results as well as mass spectrometry analyses, indicating that specific nerves running through the CA contain these neuropeptides.[6,36,37]

Remarkably, little if any qualitative differences can be observed between the >30 year old FFPE tissue detected peptides and those that can be imaged in freshly prepared unfixed cockroach CC/CA[18,26] or that have recently have been reported detectable in *P. americana* CC/CA cryosections.[38] In a few sections of the >30 years old FFPE tissue preparation, the well-known cockroach pentapeptide neurohormone, proctolin, which was not reported in our previous publication,[26] was detected. Proctolin was the very first insect neuropeptide (a myotropic peptide) to be sequenced (RYLPT) after a laborious isolation effort starting from 125 kg of adult American cockroaches.[39] Ions associated with

DOI: 10.1021/acs.analchem.8b01838
Anal. Chem. 2018, 90, 9272−9280

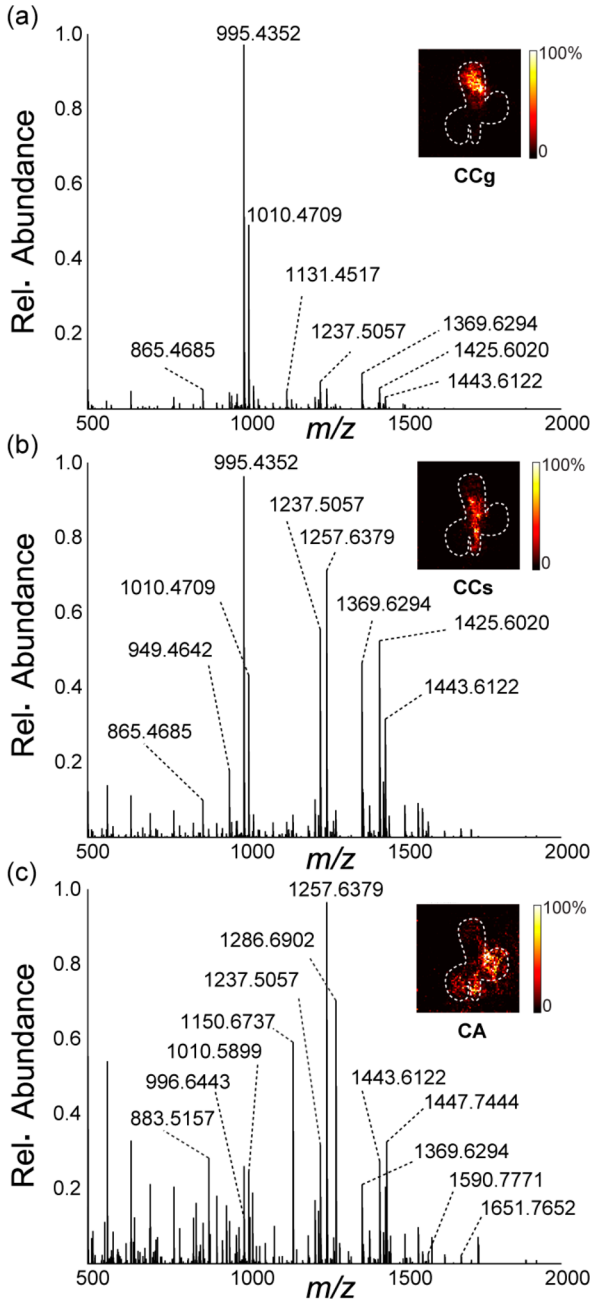

Figure 3. Representative PCA cluster mean spectra based on tissue structure-associated data clustering observed in Figure 2 for (a) CCg region, (b) CCs lobe, and (c) CA region in *P. americana* retrocerebral complex.

proctolin (m/z 649.3668; $[M + H]^+$) were found to be present exclusively in sections containing a small cross section through the insect's recurrent nerve (which was not included in the whole mount tissue preparation analyzed in our work mentioned above[18,26]). Indeed, the nervus recurrens, part of the cockroach stomatogastric nervous system, is known to transport proctolin from the frontal ganglion further into the body.[40] None of the above typical neuropeptide signals are observed in the non-neuronal tissues present in the histological section, such as the insect foregut epithelium and visceral muscle, as well as its tracheal system (see also Figure 4a).

Using a high-throughput MALDI-ToF instrument, 26 FFPE serial sections from a 30 year old paraffin block containing a *P. americana* retrocerebral complex (deposited on a single glass slide) were analyzed by MALDI-MSI at 50 μm spatial resolution (Figure 4). Figure 4a shows the distribution of three selected endogenous peptides: Pea-PK-3, Pea-CAH-1, and corazonin as overlays on an optical image of the tissue poststained with H&E. The images demonstrate that the sample preparation method was effective across multiple tissue sections for the detection of endogenous peptides from FFPE tissue with minimal delocalization. The observed localization of all the known CC/CA neuropeptides detected (which exhibit distinct spatial distributions within each section, and at various depths throughout the volume of the retrocerebral complex (circled in black)) is limited to the neurosecretory tissue, as the neighboring foregut tissue did not yield signals associated with known neuropeptide ions. Peaks for all the neuropeptides listed in Table 1 were detected at various positions throughout the 3D volume of the retrocerebral complex with a representative positive-ion mode single pixel spectrum shown in Figure 4b.

DISCUSSION

More than a decade ago, the group of Salzet and Fournier reported "trypsin-free" imaging of a neuropeptide from young FFPE material prepared with the "reactive" MALDI matrix 2,4-dinitrophenylhydrazine.[12] However, they were unable to image neuropeptides in older material, concluding that FFPE neuropeptide imaging by MALDI-MSI only works using a reactive matrix, and only on tissues less than 1 year after embedding.

Following this work, Chaurand et al.[41] as well as Gray et al.[42] evaluated alcohol-based alternative fixation methods that were amenable to protein MSI as an alternative to cryopreservation. The former study (analyzing mouse lung, kidney, brain and liver) employed 70% ethanol, and the latter reported MALDI-ToF data from chick heart tissue fixed in acidified alcohol.[41] Chaurand et al.[41] extensively addressed the considerable wash-out of proteins during EtOH fixation, and both reports show data of "protein-like" MALDI-MS peaks (between m/z 2000–50000) in ethanol-preserved paraffin-embedded (EPPE) material. These studies demonstrated that a considerable proportion of the peptides and low molecular weight proteins were extracted from the tissue during ethanol "fixation", implying that this methodology is not optimal for small, low-abundant endogenous peptide imaging. It has also been stated that the chemical crosslinking by formaldehyde fixation renders samples unsuitable for MSI analysis of proteins, unless enzymatic digestion is included in the protocol. Based on those findings, recent studies investigating neuropeptides within the retrocerebral complexes of *P. americana* using MSI have targeted freshly frozen and cryo-embedded tissues. As such the studies by the Predel group[38] not only confirm and validate our previous study on fresh cockroach neuropeptide MSI,[26] but also our current work. More extensive lists of *P. americana* neuropeptide sequences identified from cockroach neuronal tissues different than the currently examined CC/CA have been reported previously.[32,36]

The major novelty of the present work is the finding that endogenous secretory peptides such as authentic neuropeptides can be analyzed by MSI in formaldehyde-fixed material that is paraffin-embedded for several years and stored at ambient temperature for the duration. Exemplar tissues investigated in this paper included neurosecretory glands containing a set of known neuropeptides reported above. Our

DOI: 10.1021/acs.analchem.8b01838
Anal. Chem. 2018, 90, 9272–9280

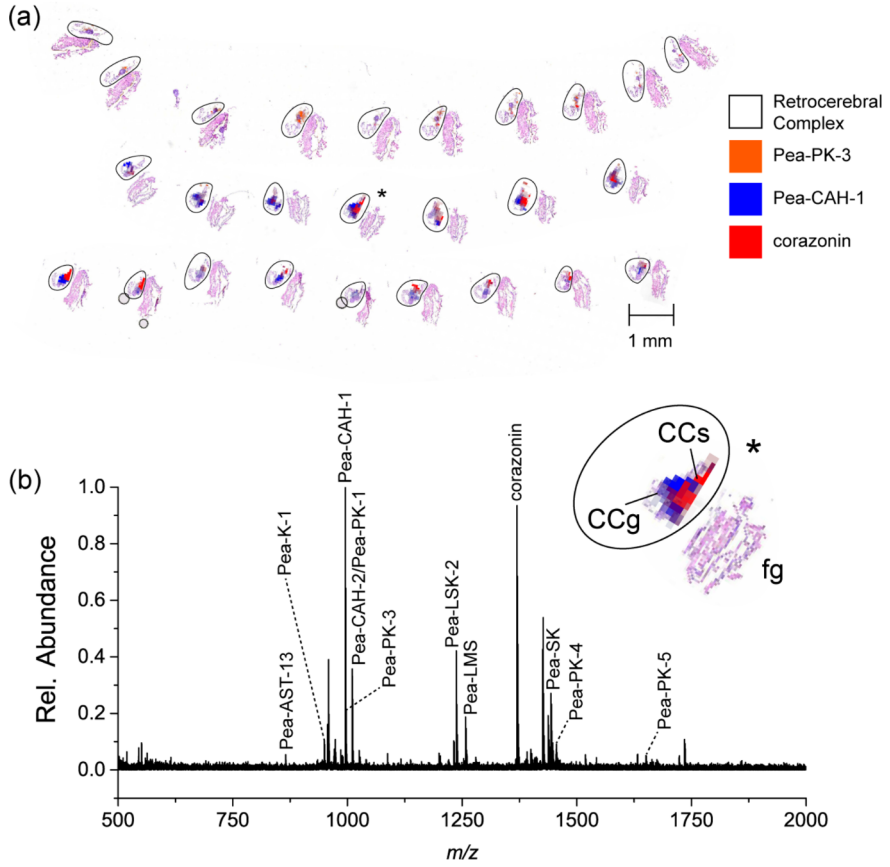

Figure 4. (a) MALDI-ToF MS images of 20 μm-thick consecutive sections obtained from retrocerebral complex of *P. americana* showing three selected neuropeptides: Pea-PK (orange square), Pea-CAH-1 (blue square), and corazonin (red square), as overlays on optical image of tissues poststained with H&E. Retrocerebral complex tissue regions are circled in black; scale bar: 1 mm. (b) Positive-ion mode single pixel MALDI-ToF spectrum acquired from retrocerebral complex of *P. americana*. Inset: tissue section used to acquire spectrum as shown from series of sections analyzed in (a) and denoted with (*). Corpus cardiacum glandular lobe (CCg), neuroheamal storage site (CCs), and foregut (fg) are annotated for orientation purposes.

data indicate that in the model system investigated, the majority of the neuropeptides detectable in fresh or freshly frozen tissue are similarly detected as neuropeptide ion peaks in 30 year-old FFPE tissues. This confirms that several neuropeptides remain fully preserved in the tissue "unharmed", that is, not degraded by catabolic enzymes.

In principle this is not surprising, as neuropeptides can be detected in FFPE tissues with antibodies in immunohistochemical (IHC) analyses. The rinsing and dehydration steps after formaldehyde fixation and prior to paraffin embedding, therefore, do not cause a complete removal of small (neuro)peptides or chemical alteration of the relevant part of a peptide required for neuropeptide antibody recognition.

Accordingly, the general belief that all peptides become inaccessible for MSI in tissues following formalin-fixation, without first performing in situ digestion,[10] is disproven in this study. In view of the underlying chemistry of formaldehyde crosslinking, we rationalize this as follows.[43] Not all amino acid residues within a peptide sequence react with the smallest aldehyde to the same extent. Especially, the amino groups covalently bind to formaldehyde, that is, the amino terminus and the amino groups in the amino acid side chains, in particular, the ϵ-amino function in Lys residues.[43,44] Like most (bio)chemical reactions, however, the formaldehyde-fixation is an equilibrium reaction. Hence, for each of the formaldehyde-reactive amino acid residues, a fraction is not crosslinked. Thus, for peptide species with a short sequence, especially with only one or less Lys residues and lacking a free amino terminus, it is likely that the proportion of molecules that are not fully crosslinked is substantial, and able to be detected with sensitive MS instrumentation.

In view of the above, our method is expected to have a bias in favor of shorter peptides with less Lys-residues. Recent statistics of the UniProt/TrEMBL sequence database (UniProt Release 2017_12; http://www.uniprot.org/statistics/TrEMBL), indicate that the overall frequency of Lys residues in a protein is 5.0%, which means that on average each 20th amino acid residue in a protein is a Lys. Longer proteins with more than one Lys residue have a greater probability to be more extensively crosslinked and are, therefore, more challenging to detect by mass spectrometry in FFPE samples.

In the same context, we remark that of the peptides we successfully imaged in this study (Table 1), none appears to contain a lysine, and a significant number have a blocked amino terminus (pQ, pyroglutamate). Not surprisingly, all peptides positively identified in this study have <20 residues (with Pea-PK-6, the longest known neuropeptide imaged in this study, totaling 14 residues).

Following the same logic, it is highly unlikely that large polypeptides and proteins would freely exist in FFPE tissue. Such multiple crosslinking through formaldehyde fixation is thought to be one of the mechanisms by which tissues can be

DOI: 10.1021/acs.analchem.8b01838
Anal. Chem. 2018, 90, 9272−9280

preserved for ages. Since the typical proteases, peptidases, and other catabolic/protein modifying enzymes are invariably large proteins which easily contain more than ∼300 amino acid residues, they will be firmly crosslinked in FFPE material, and, therefore, unable to exhibit any enzyme activity. Endogenous peptides, although natively chemically very labile, will, therefore, "survive" unmodified or catabolized. As such, rather than obstructing (top-down) peptidomics analyses, formalin fixation may well be an efficient catabolic enzyme deactivating sample preparation/stabilization step if one wants to preserve small peptides.

CONCLUSION

We have developed an MSI protocol that enabled the localization of secretory endogenous (neuro)peptides on more than 30 years old FFPE tissue. We conclude that the covalent formaldehyde crosslinking of small neuropeptides (especially, but not exclusively, amino terminally blocked and poor in lysine content) with other biomolecules is not 100% complete. At the same time, the washing and dehydration steps prior to paraffin embedding do not cause a complete removal of small noncrosslinked (neuro)peptides, and the risk to remove peptides through the necessary (but maximally reduced) deparaffinization and rehydration steps may be overrated. The method does not include laborious in situ protease digestion or antigen retrieval steps that are known to negatively interfere with the detection of low abundant endogenous peptides. Our current work unequivocally indicates that lysine-low peptides as large as 14 amino acid residues can be structurally characterized and imaged in FFPE material stored for 30 years. The method is likely to be universally applicable to biology in general and to the study of health and disease. The results of our analyses using de novo sequencing assisted database searching indicates that the newly described workflow could potentially be used as a discovery tool to image previously undescribed (neuro)peptides. Excitingly, this method has the potential to unlock part of the biologically relevant molecular information "fixed" in the many millions of FFPE tissue blocks, which are catalogued in biobanks of hospitals, research institutes, and even museums of natural history worldwide.

ASSOCIATED CONTENT

Supporting Information

The Supporting Information is available free of charge on the ACS Publications website at DOI: 10.1021/acs.analchem.8b01838.

SI Figure 1: Tandem mass spectra of collision-induced dissociation (CID) experiments performed in the ion-trap analyzer for peptides detected at high enough signal in FFPE cockroach retrocerebral complex tissue section. Sequence-specific fragment ion peaks confirming the respective peptides' primary structure are annotated (PDF).

AUTHOR INFORMATION

Corresponding Author

*E-mail: p.verhaert@maastrichtuniversity.nl; peter.verhaert@proteoformix.com.

ORCID

Martin R. L. Paine: 0000-0002-9360-1969

Ron M. A. Heeren: 0000-0002-6533-7179

Peter D. E. M. Verhaert: 0000-0002-6921-087X

Notes

The authors declare no competing financial interest.

ACKNOWLEDGMENTS

This research has been made possible with the support of the Dutch Province of Limburg through the LINK Program. Part of the research was funded by ITEA and RVO (Project Number ITEA151003/ITEA 14001). The authors are indebted to Prof. Dr. Axel zur Hausen (chairman Department of Pathology, University Hospital Maastricht) for providing access to one of their microtomes. P.V. would like to dedicate this paper to his first histology and insect endocrinology teachers, respectively, Prof. Dr. M. Quaghebeur (who sadly passed away earlier this year) and Prof. Dr. Ir. A. De Loof, both emeriti from the Zoological Institute at the University of Leuven, Belgium.

REFERENCES

(1) Clemmons, D. R.; Van Wyk, J. J. *J. Clin. Invest.* **1985**, *75*, 1914−1918.

(2) Lehrer, R. I.; Ganz, T. *Curr. Opin. Hematol.* **2002**, *9*, 18−22.

(3) Mahlapuu, M.; Håkansson, J.; Ringstad, L.; Björn, C. *Front. Cell. Infect. Microbiol.* **2016**, *6*, 194.

(4) Nussey, S. S.; Whitehead, S. A. *Endocrinology: An Integrated Approach*; CRC Press, 2013.

(5) Romanova, E. V.; Lee, J. E.; Kelleher, N. L.; Sweedler, J. V.; Gulley, J. M. *AAPS J.* **2010**, *12*, 443−454.

(6) Predel, R. *J. Comp. Neurol.* **2001**, *436*, 363−375.

(7) Weiner, R. I.; Ganong, W. F. *Physiol. Rev.* **1978**, *58*, 905−976.

(8) Stauber, J.; Lemaire, R.; Franck, J.; Bonnel, D.; Croix, D.; Day, R.; Wisztorski, M.; Fournier, I.; Salzet, M. *J. Proteome Res.* **2008**, *7*, 969−978.

(9) Fox, C. H.; Johnson, F. B.; Whiting, J.; Roller, P. P. *J. Histochem. Cytochem.* **1985**, *33*, 845−853.

(10) Casadonte, R.; Caprioli, R. M. *Nat. Protoc.* **2011**, *6*, 1695−1709.

(11) Fridjonsdottir, E.; Nilsson, A.; Wadensten, H.; Andrén, P. E. In *Peptidomics: Methods and Strategies*; Schrader, M., Fricker, L., Eds.; Springer: New York, NY, 2018; pp 41−49.

(12) Lemaire, R.; Desmons, A.; Tabet, J. C.; Day, R.; Salzet, M.; Fournier, I. *J. Proteome Res.* **2007**, *6*, 1295−1305.

(13) Ly, A.; Buck, A.; Balluff, B.; Sun, N.; Gorzolka, K.; Feuchtinger, A.; Janssen, K. P.; Kuppen, P. J.; van de Velde, C. J.; Weirich, G.; Erlmeier, F.; Langer, R.; Aubele, M.; Zitzelsberger, H.; McDonnell, L.; Aichler, M.; Walch, A. *Nat. Protoc.* **2016**, *11*, 1428−1443.

(14) Bruand, J.; Sistla, S.; Mériaux, C.; Dorrestein, P. C.; Gaasterland, T.; Ghassemian, M.; Wisztorski, M.; Fournier, I.; Salzet, M.; Macagno, E.; Bafna, V. *J. Proteome Res.* **2011**, *10*, 1915−1928.

(15) Zhang, Y.; Buchberger, A.; Muthuvel, G.; Li, L. *Proteomics* **2015**, *15*, 3969−3979.

(16) DeKeyser, S. S.; Kutz-Naber, K. K.; Schmidt, J. J.; Barrett-Wilt, G. A.; Li, L. *J. Proteome Res.* **2007**, *6*, 1782−1791.

(17) Brand, G. D.; Krause, F. C.; Silva, L. P.; Leite, J. R. S. A.; Melo, J. A. T.; Prates, M. V.; Pesquero, J. B.; Santos, E. L.; Nakaie, C. R.; Costa-Neto, C. M.; Bloch, C. *Peptides* **2006**, *27*, 2137−2146.

(18) Verhaert, P. D. E. M.; Pinkse, M. W. H.; Prieto-Conaway, M. C.; Kellmann, M. *Peptidomics*; John Wiley & Sons, Inc., 2007; pp 25−54.

(19) Chatterji, B.; Dickhut, C.; Mielke, S.; Krüger, J.; Just, I.; Glage, S.; Meier, M.; Wedekind, D.; Pich, A. *Proteomics* **2014**, *14*, 1674−1687.

(20) Källback, P.; Shariatgorji, M.; Nilsson, A.; Andrén, P. E. *J. Proteomics* **2012**, *75*, 4941−4951.

DOI: 10.1021/acs.analchem.8b01838
Anal. Chem. 2018, 90, 9272−9280

(21) Hanrieder, J.; Ljungdahl, A.; Fälth, M.; Mammo, S. E.; Bergquist, J.; Andersson, M. *Mol. Cell. Proteomics* **2011**, *10*, M111.009308.
(22) Altelaar, A. F. M.; Taban, I. M.; McDonnell, L. A.; Verhaert, P. D. E. M.; de Lange, R. P. J.; Adan, R. A. H.; Mooi, W. J.; Heeren, R. M. A.; Piersma, S. R. *Int. J. Mass Spectrom.* **2007**, *260*, 203−211.
(23) Guenther, S.; Römpp, A.; Kummer, W.; Spengler, B. *Int. J. Mass Spectrom.* **2011**, *305*, 228−237.
(24) Ong, T.-H.; Romanova, E. V.; Roberts-Galbraith, R. H.; Yang, N.; Zimmerman, T. A.; Collins, J. J.; Lee, J. E.; Kelleher, N. L.; Newmark, P. A.; Sweedler, J. V. *J. Biol. Chem.* **2016**, *291*, 8109−8120.
(25) Gemperline, E.; Keller, C.; Jayaraman, D.; Maeda, J.; Sussman, M. R.; Ané, J.-M.; Li, L. *J. Proteome Res.* **2016**, *15*, 4403−4411.
(26) Verhaert, P. D.; Pinkse, M. W.; Strupat, K.; Conaway, M. C. P. In *Mass Spectrometry Imaging; Methods in Molecular Biology (Methods and Protocols)*; Rubakhin, S., Sweedler, J., Eds.; Humana Press: Totowa, NJ, 2010.
(27) Verhaert, P.; De Loof, A.; Huybrechts, R.; Delang, I.; Theunis, W.; Clottens, F.; Schoofs, L.; Swinnen, K.; Vandesande, F. *J. Neurosci. Methods* **1986**, *17*, 261−268.
(28) Belov, M. E.; Ellis, S. R.; Dilillo, M.; Paine, M. R. L.; Danielson, W. F.; Anderson, G. A.; de Graaf, E. L.; Eijkel, G. B.; Heeren, R. M. A.; McDonnell, L. A. *Anal. Chem.* **2017**, *89*, 7493−7501.
(29) Eijkel, G. B.; Kükrer Kaletaş, B.; van der Wiel, I. M.; Kros, J. M.; Luider, T. M.; Heeren, R. M. A. *Surf. Interface Anal.* **2009**, *41*, 675−685.
(30) Trede, D.; Schiffler, S.; Becker, M.; Wirtz, S.; Steinhorst, K.; Strehlow, J.; Aichler, M.; Kobarg, J. H.; Oetjen, J.; Dyatlov, A.; Heldmann, S.; Walch, A.; Thiele, H.; Maass, P.; Alexandrov, T. *Anal. Chem.* **2012**, *84*, 6079−6087.
(31) Zhang, J.; Xin, L.; Shan, B.; Chen, W.; Xie, M.; Yuen, D.; Zhang, W.; Zhang, Z.; Lajoie, G. A.; Ma, B. *Mol. Cell. Proteomics* **2012**, *11*, M111.010587.
(32) Neupert, S.; Fusca, D.; Schachtner, J.; Kloppenburg, P.; Predel, R. *J. Comp. Neurol.* **2012**, *520*, 694−716.
(33) Siegert, K. J.; Morgan, P. J.; Mordue, W. *Insect Biochem.* **1986**, *16*, 365−371.
(34) Adams, M. E. In *Cockroaches as Models for Neurobiology: Applications in Biomedical Research*; Huber, I., Masler, E. P., Rao, B. R., Eds.; CRC Press, 1990; pp 3−34.
(35) Raabe, M. *Insect Neurohormones*; Plenum Press: New York and London, 1982.
(36) Predel, R.; Gade, G. *Peptides* **2005**, *26*, 3−9.
(37) Predel, R.; Eckert, M.; Pollák, E.; Molnár, L.; Scheibner, O.; Neupert, S. *J. Comp. Neurol.* **2007**, *500*, 498−512.
(38) Ly, A.; L, R.; Liessem, S.; Becker, M.; S.-O, D.; Predel, R. *65th ASMS Conference on Mass Spectrometry and Allied Topics*; Indianapolis, IN, U.S.A.; June 4−8, 2017, ASMS, 2017.
(39) Brown, B. E.; Starratt, A. N. *J. Insect Physiol.* **1975**, *21*, 1879−1881.
(40) Bell, W. J.; Adivodi, K. G. *The American Cockroach*; Chapmen and Hall: London, 1981.
(41) Chaurand, P.; Latham, J. C.; Lane, K. B.; Mobley, J. A.; Polosukhin, V. V.; Wirth, P. S.; Nanney, L. B.; Caprioli, R. M. *J. Proteome Res.* **2008**, *7*, 3543−3555.
(42) Grey, A. C.; Gelasco, A. K.; Section, J.; Moreno-Rodriguez, R. A.; Krug, E. L.; Schey, K. L. *Anat. Rec.* **2010**, *293*, 821−828.
(43) Klockenbusch, C.; O'Hara, J. E.; Kast, J. *Anal. Bioanal. Chem.* **2012**, *404*, 1057−1067.
(44) Metz, B.; Kersten, G. F.; Hoogerhout, P.; Brugghe, H. F.; Timmermans, H. A.; de Jong, A.; Meiring, H.; ten Hove, J.; Hennink, W. E.; Crommelin, D. J.; Jiskoot, W. *J. Biol. Chem.* **2004**, *279*, 6235−6243.

DOI: 10.1021/acs.analchem.8b01838
Anal. Chem. 2018, 90, 9272−9280